

Inference of time-ordered multibody interactions

Unai Alvarez-Rodriguez,¹ Luka V. Petrović,¹ and Ingo Scholtes^{1,2}

¹University of Zurich, Zürich, Switzerland

²Julius-Maximilians-Universität Würzburg, Würzburg, Germany

(Dated: November 30, 2021)

We introduce time-ordered multibody interactions to describe complex systems manifesting temporal as well as multibody dependencies. First, we show how the dynamics of multivariate Markov chains can be decomposed in ensembles of time-ordered multibody interactions. Then, we present an algorithm to extract combined interactions from data and a measure to characterize the complexity of interaction ensembles. Finally, we experimentally validate the robustness of our algorithm against statistical errors and its efficiency at obtaining simple interaction ensembles.

Earth’s climate, the traffic in a giant metropolis, and even a baroque musical composition are all examples of complex systems. They are composed of multiple elements with different types of interactions and elusive dynamical laws [1–3]. The efforts to understand those laws have prompted the advance of network science in the last few decades. The journey started with standard networks [4–6], continued with multilayer and multiplex networks [7, 8], and has brought us to the time of higher-order networks [9–17]. Over time, we have learned to impose weaker assumptions upon our models and thus to describe more complex interactions.

Lately, the community has primarily focused on two types of interactions: multibody interactions and time-ordered interactions. The former are modeled with hypergraphs and the latter are modeled with higher-order Markov chains. Each of them violates a different assumption of standard networks: multibody interactions violate the assumption that system dynamics can be explained solely with dyadic interactions; time-ordered interactions violate the Markov assumption [18, 19]. However, real systems may violate both assumptions, invalidating either modeling approach. This situation leads to multiple open questions. How can we analyze systems that manifest interactions that are both time-ordered and multibody? More specifically, how can we formalize such interactions and infer them from data? How can we use time-ordered multibody interactions to explain system dynamics? There are preliminary efforts in combining time-ordered and multibody interactions by means of models for synchronization [20], contagion [21] and consensus dynamics [22]. However a general formalism is yet to be found.

In this letter, we propose a unified methodology for scenarios in which multibody and time-ordered dependencies coexist. First, we introduce parsimonious models of time-ordered multibody interactions. Then, we present an algorithm to decompose the system dynamics into an ensemble of interactions. Last, we introduce a measure to characterise the complexity of interaction ensembles. We show how the integration of time-ordered and multibody interactions enables a better description of real world sys-

tems than current modeling paradigms.

Let S be a closed system of N nodes $n \in \mathcal{N}$. Each node n is constrained to a finite set of states, called alphabet X_n with cardinality $|X_n|$. We denote the state of each node n at a given time t with $s_n(t)$, and the state of the whole system with $\mathbf{s}(t) = (s_n(t))_{n \in \mathcal{N}}$. Thus, the alphabet of the whole system is $X = \prod_{n \in \mathcal{N}} X_n$, where \prod denotes Cartesian product. We observe the system in an interval (t_0, t_{end}) and collect sequences of system states $\mathbf{D} = (\mathbf{s}(\tau))_{\tau=t_0}^{t_{\text{end}}}$ and element states $\mathbf{D}_n = (s_n(\tau))_{\tau=t_0}^{t_{\text{end}}}$.

We can model the dynamics of S as a higher-order Markov chain with memory m : the transition probability to a state $x \in X$ depends on the previous m states $\bar{x} \in |X|^m$. The transition probabilities $\pi(x|\bar{x})$ are encoded in matrix elements $T_{x\bar{x}}$ of transition matrices \mathbf{T} with dimensions $|X| \times |X|^m$. One can infer the transition matrix \mathbf{T} for different Markov orders m using the temporal data \mathbf{D} , and select the Markov order that provides the best predictability-parsimony balance [23–25].

Higher-order Markov chains model the dynamics of S as a function of all nodes at all times and thus one cannot analyze node interdependencies in isolation. Therefore, we deviate from this modelling approach, and define time-ordered multibody interactions that depend only on last q_n states of node n . We denote a group of q_n successive temporal states of node n with tuples $\mathbf{G}_n^{q_n}(t) := (s_n(\tau))_{\tau=t-q_n+1}^t$. If q_n is zero, $\mathbf{G}_n^{q_n}(t)$ denotes an empty tuple. We then construct a vector $\mathbf{q} = (q_n)_{n \in \mathcal{N}}$ and denote groups of variables for the whole system $\mathbf{G}^{\mathbf{q}}(t) := (\mathbf{G}_n^{q_n}(t))_{n \in \mathcal{N}}$. States of $\mathbf{G}^{\mathbf{q}}(t)$ take values in alphabet $X^{\mathbf{q}} := \prod_{n \in \mathcal{N}} X_n^{q_n}$. Before defining time-ordered multibody interactions, we emphasize that in our notation Markov chains with memory m model $\mathbf{s}(t) = \mathbf{G}^{\mathbf{1}}(t)$ given the history $\mathbf{G}^{\mathbf{m}}(t-1)$, where $\mathbf{1}$ and \mathbf{m} are vectors with all components 1 and m , respectively. The transition probabilities then depend on $o := m+1$ system states, amounting to a total oN time variables $\mathbf{G}^{\mathbf{o}}(t)$.

The core of our formalism are time-ordered multibody interactions, which depend only on a subset of the $\mathbf{G}^{\mathbf{o}}(t)$ variables of higher-order Markov chains. A time-ordered multibody interaction \mathcal{A} of type \mathbf{q} , $0 \leq q_n \leq o$, models the probability of $\mathbf{s}(t)$ given history $\mathbf{G}^{\mathbf{m}}(t-1)$ as

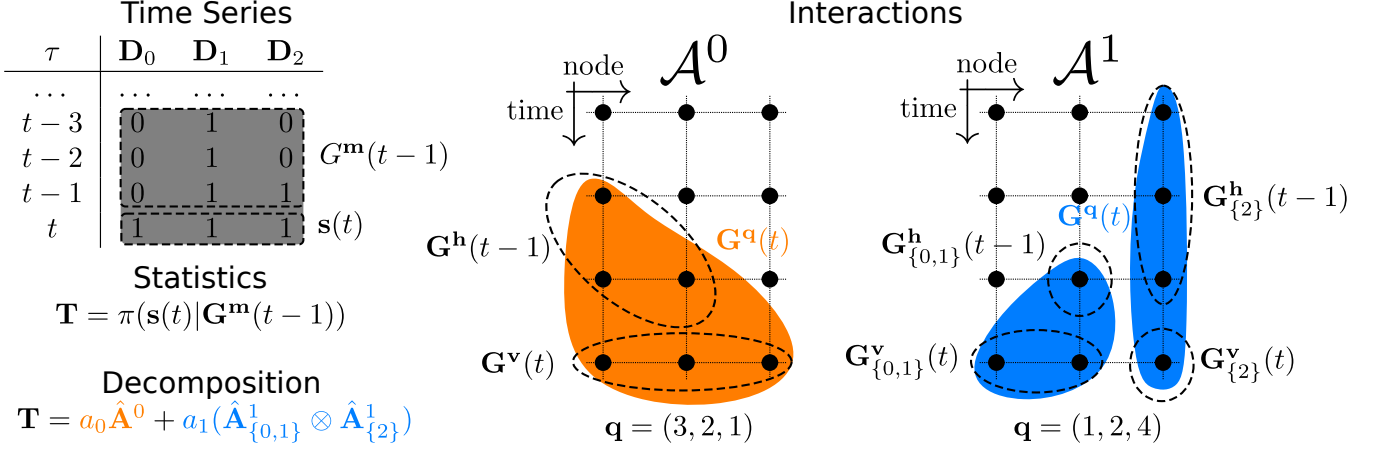


FIG. 1: We are presented the task to explain the dynamics of a system of $N = 3$ nodes from their temporal data \mathbf{D} . We first compute a higher-order Markov chain of memory $m = 3$ and collect the transition probabilities in a matrix \mathbf{T} , which predicts the joint node state $\mathbf{s}(t)$ as a function of the previous three states $\mathbf{G}^m(t-1)$. We then decompose \mathbf{T} as a convex sum of time-ordered multibody interactions \mathcal{A}^i . An interaction of type \mathbf{q} models the dynamics as a function of the group of system variables $\mathbf{G}^q(t)$, which contains q_n variables of each node n . $\mathbf{G}^q(t)$ is divided in $\mathbf{G}^v(t)$ and $\mathbf{G}^h(t-1)$ that account respectively for row and column variables of interaction transition matrices $\hat{\mathbf{A}}^i$. The interaction \mathcal{A}^1 is separated into two dynamically independent subsystem interactions $\mathcal{A}^1_{\{0,1\}}$ and $\mathcal{A}^1_{\{2\}}$.

a function of variables $\mathbf{G}^q(t)$ and independent of other variables. We separate the variables $\mathbf{G}^q(t)$ in two groups: variables $\mathbf{G}^v(t)$ describing nodes at time t and variables $\mathbf{G}^h(t-1)$ describing their history. Here, the components of \mathbf{v} are $v_n = 0$ when $q_n = 0$ and $v_n = 1$ when $q_n > 0$; the vector \mathbf{h} contains history lengths $\mathbf{h} = \mathbf{q} - \mathbf{v}$. See Fig. 1 for an example of an interaction in a system of three nodes, and corresponding $\mathbf{G}^v(t)$ and $\mathbf{G}^h(t-1)$. The variables $\mathbf{G}^v(t)$ are modeled with a multinomial distribution that depends on the history $\mathbf{G}^h(t-1)$. The state of $\mathbf{G}^v(t)$ takes values $y \in X^v$, and the state of $\mathbf{G}^h(t-1)$ takes values $\bar{y} \in X^h$. The transition probabilities from \bar{y} to y are encoded in the transition matrix $A_{y\bar{y}}$ of interaction \mathcal{A} . For nodes where $q_n = 0$, the probabilities of $s_n(t)$ do not depend on any variable, and thus they are uniform. In summary, an interaction \mathcal{A} models the dynamics as:

$$\pi(\mathbf{s}(t)|\mathbf{G}^m(t-1), \mathcal{A}) = \frac{A_{y\bar{y}}}{\prod_{q_n=0} |X_n|}. \quad (1)$$

While the transition matrix \mathbf{T} has $|X| \times |X|^M = \prod_n |X_n|^o$ elements, the interaction \mathcal{A} of type \mathbf{q} has only $|X^v| \times |X^h| = \prod_{n \in \mathcal{N}} |X_n|^{q_n}$ parameters. Therefore, interactions produce a parsimonious model of the system dynamics. With this, we have formally introduced time-ordered multibody interactions, and we now discuss how we can use them to decompose the dynamics of S .

The aim of our decomposition is to explain the dynamics in terms of the simplest possible interactions. Therefore, we organize time-ordered multibody interactions in a hierarchy by their complexity. We define the interac-

tion order ω of interaction type \mathbf{q} as $\omega = \sum_{n \in \mathcal{N}} q_n$, that counts the number of variables on which the interaction depends. Moreover, interactions are nested models: an interaction \mathcal{A} of type \mathbf{q} can be nested in (or represented with) an interaction \mathcal{A}' of type \mathbf{q}' iff $\forall n : q_n \leq q'_n$. Intuitively, if variables of \mathcal{A} are a subset of variables of \mathcal{A}' , \mathcal{A} can be nested in \mathcal{A}' . The relation of nestedness over the set of interaction types naturally defines a partial order, which is commonly depicted with a Hasse diagram. In the Hasse diagram on Fig 2, two interaction types are connected as long as they are nested and separated by one interaction order ω . For example, an interaction of type $(2, 1, 0)$ (leftmost type in fourth row of Fig. 2) models the dynamics of S as a function of $s_0(t)$, $s_0(t-1)$, and $s_1(t)$. Thus, it can be nested in any interaction type that includes these variables. The interaction type \mathbf{o} , which corresponds to a Markov chain on S , is particularly important for the decomposition because any other type of interaction can be nested in it. When we nest an interaction \mathcal{A} in type \mathbf{o} , we denote the resulting interaction with $\hat{\mathcal{A}}$ and its transition matrix with $\hat{\mathbf{A}}$.

The decomposition algorithm has two parts: in the first part we decompose the transition matrix \mathbf{T} in an ensemble of time-ordered interactions; in the second part, we decompose the time-ordered interactions in subsystem interactions. Formally, in the first part we find the interaction coefficients a_i and matrices $\hat{\mathbf{A}}^i$ (here, i is an upper index) such that the matrix \mathbf{T} can be expanded as a convex sum: $\mathbf{T} = \sum_i a_i \hat{\mathbf{A}}^i$. The algorithm repeatedly extracts interactions from \mathbf{T} . Starting at $\omega = 0$,

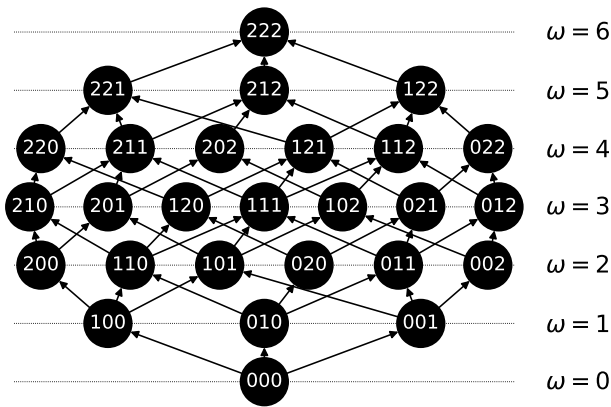


FIG. 2: Hasse diagram of time-ordered multibody interactions for a system of three nodes and memory equal to one. Interaction types are depicted as vertices \mathbf{q} , and arranged according to their interaction order ω . If there is a path from \mathbf{q} to \mathbf{q}' , then every interaction of type \mathbf{q} can be expressed as an interaction of type \mathbf{q}' .

it randomly explores all interactions at ω before proceeding with $\omega + 1$. Let us assume we have already extracted i interactions from \mathbf{T} and that $\tilde{\mathbf{T}}$ is the remainder: $\tilde{\mathbf{T}} = \mathbf{T} - \sum_{j=0}^{i-1} a_j \hat{\mathbf{A}}^j$. For the next interaction \mathcal{A}^i , the algorithm finds the transition matrix \mathbf{A}^i such that the corresponding coefficient a_i is maximal and $\tilde{\mathbf{T}} - a_i \hat{\mathbf{A}}^i$ doesn't have negative elements. The first part finishes when either $\tilde{\mathbf{T}}$ is a matrix of zeros, or, equivalently, when the sum of the interaction coefficients is one. See SM for the details.

The second part of the algorithm identifies statistically independent subsystems and decomposes the interactions into “subsystem interactions”. Formally, subsystem interactions are interactions defined on a subset of nodes. Let $\mathcal{P}(\mathcal{N})$ be a partition of \mathcal{N} , and $\mathcal{B} \in \mathcal{P}(\mathcal{N})$ be a subset of nodes $\mathcal{B} \subset \mathcal{N}$. If x is a state of nodes \mathcal{N} and \bar{x} is the history of the state, we denote the corresponding state of the nodes \mathcal{B} with $z_{\mathcal{B}}$ and their corresponding history $\bar{z}_{\mathcal{B}}$. We say that interaction \mathcal{A} has a subsystem interaction partition $\mathcal{P}(\mathcal{N})$ iff

$$\pi(x|\bar{x}, \mathcal{A}) = \prod_{\mathcal{B} \in \mathcal{P}(\mathcal{N})} \pi(z_{\mathcal{B}}|\bar{z}_{\mathcal{B}}, \mathcal{A}_{\mathcal{B}}) \quad (2)$$

For instance, nodes with $q_n = 0$ are obvious examples of independent subsystem interactions.

We identify subsystem interactions from an interaction \mathcal{A} by iteratively factorizing its transition matrix as a tensor product. First, we factor out each node n that is modeled with a uniform distribution $q_n = 0$. We thus obtain the partition with one-element subsets for nodes n with $q_n = 0$, and a single subset containing the remaining nodes. Then, we iteratively search for two-group partitions of the subsets with more than one element. We

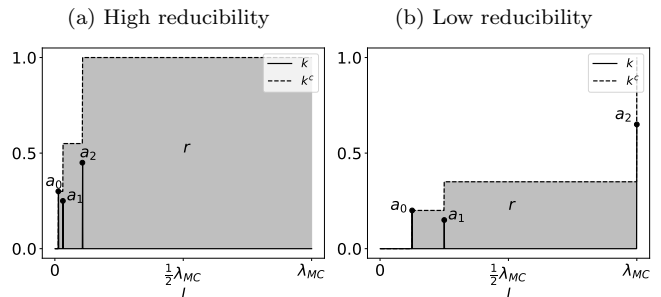


FIG. 3: Complexity measures $k(l)$, $k^c(l)$ and r for (a) high reducibility and (b) low reducibility systems. Here $\lambda(\mathcal{A})$ is the number of free parameters of an interaction, $k(l)$ weights how likely is to have an interaction with l parameters in an interaction ensemble, and $k^c(l)$ is the cumulative of $k(l)$. The reducibility r is the share of area under $k^c(l)$, and encodes the relative reduction in the average number of parameters per interaction of an ensemble. The ensemble in (a) has the same predictive power as \mathbf{T} even if its matrices contain 94% less parameters on average.

stop when we cannot find a valid partition of any subset. See SM for the details on the subsystem interaction factorization and an example.

Having discussed the formalism of time-ordered multibody interactions, and the algorithm to extract them from data, we now focus on the complexity of interaction ensembles. We note that the expansion of the transition matrix \mathbf{T} is not unique, as it can be reconstructed with different ensembles of interactions and interaction coefficients. Ideally we are looking for an ensemble with the lowest possible complexity. We then need a principled way of measuring such complexity for different combinations of interactions and subsystem interactions.

To quantify the complexity of an ensemble of interactions, we introduce the measure of reducibility. Let us denote the number of degrees of freedom of an interaction \mathcal{A} with $\lambda(\mathcal{A})$. When interactions have no subsystem interactions, $\lambda(\mathcal{A})$ is simply $(|X^{\mathbf{v}}| - 1)|X^{\mathbf{h}}|$ due to the normalization of stochastic matrices. If \mathcal{A} has subsystem interactions, $\lambda(\mathcal{A})$ is given by the sum of their parameters $\lambda(\mathcal{A}) = \sum_{\mathcal{B}} \lambda(\mathcal{A}_{\mathcal{B}})$. We call the ensemble reducible if it is dominated by the simple interactions, and we call it irreducible if it is dominated by the complex interactions. Formally, reducibility is defined as:

$$r = \frac{\lambda_{\text{MC}} - \sum_i a_i \lambda(\mathcal{A}^i)}{\lambda_{\text{MC}}}, \quad (3)$$

where $\lambda_{\text{MC}} = (|X| - 1)|X|^m$ is the number of degrees of freedom of the Markov chain. Therefore, r accounts for the relative reduction in the average degrees of freedom per interaction when ensembles are used instead of Markov chains.

We showcase the power of this measure on the problem of lossy compression. Let us denote with $k(l)$ the weight of all interactions with l degrees of freedom: $k(l) = \sum_{\lambda(\mathcal{A}^l)=l} a_i$, and its cumulative distribution with $k^c(l)$. The value of $k^c(l)$ describes how well the interactions with less than l degrees of freedom represent the system dynamics. In Fig. 3, we depict $k(l)$ and $k^c(l)$ of a reducible and irreducible interaction ensembles. When the ensemble is reducible (panel (a)), it is dominated by the simple interactions, thus $k(l)$ peaks for small values of l , and $k^c(l)$ is high throughout the interval. When the ensemble is irreducible (panel (b)), $k(l)$ has peaks for large values of l , and $k^c(l)$ is low throughout the interval. Therefore, when an ensemble is reducible, we can choose a small l where $k^c(l)$ is high. Thus, by only using the interactions with less than l degrees of freedom, we can compress a reducible ensemble with a small loss of information. Lastly, it is worth noting that the reducibility is the share of the area under $k^c(l)$.

Finally, we present a series of experiments to validate different aspects of our contributions. We have carried out a first experiment to establish a relation between the accuracy of the algorithm and the available amount of data. Our goal here is to understand how an error in \mathbf{T} propagates to errors in a and k . We randomly generate \mathbf{T} by drawing its elements from a uniform distribution and obtain the ground truth values of interaction coefficients a and weights k . Then, we construct random sequences out of \mathbf{T} , analyse them with our algorithm, and obtain estimators $\hat{\mathbf{T}}$, \hat{a} , \hat{k} . Finally, we compute the total variation distance σ between the original indicators and the inferred ones.

Our results are reported in Fig. 4 where we explore the scalability of the algorithm as a function of N for a system with all equal alphabets $|X_n| = 2$ and order $o = 2$ (see SM for a more general selection of parameters). We consider sequences with lengths $L = \eta \prod_{i \in \mathcal{N}} |X_i|^o$, where η is a scale factor that determines the average frequency of each unique string for a uniform model. Additionally, we assume sequence's memory to be known, such that our results focus on the interaction decomposition and ignore errors due to model selection.

We observe that for regimes in which the transition

label	q	\mathcal{B}	ω	$ X^v $	$ X^h $	$\lambda(\mathcal{A})$	a
\mathcal{A}^0	210	{0, 1, 2}	3	4	2	6	0.3
\mathcal{A}^1	132	{0, 1}	4	4	4	12	0.25
		{2}	2	2	2	2	
\mathcal{A}^2	033	{0, 1, 2}	6	4	16	48	0.45

TABLE I: Interaction type \mathbf{q} , subsystem interaction partition \mathcal{B} , interaction order ω , matrix rows $|X^v|$ and columns $|X^h|$, number of parameters $\lambda(\mathcal{A})$, and coefficient a for the interaction ensemble of Fig. 3 a.

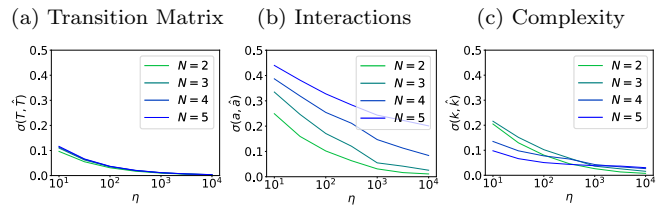


FIG. 4: We produce synthetic sequences with length $L = \eta \prod_{n \in \mathcal{N}} |X_n|^o$ and compute the statistical distance σ as a function of η between the original (a) transition matrices (b) interactions (c) weights, and the ones inferred from the data for a fixed alphabet $|X_n| = 2$ and order $o = 2$. Results reported here correspond to averages over 100 realizations for each (η, N) tuple.

matrix is able to predict accurately (Fig. 4a), and despite inferred interactions not coinciding with the ground truth (Fig. 4b), $k(l)$ can still be recovered (Fig. 4c). Errors in inferring interaction coefficients are due to the existence of multiple ensembles compatible with the same dynamics. However, this experiment reveals the capacity of the algorithm to explain the dynamics with an ensemble whose weights and reducibility are close to the ground truth values. Therefore, the protocol is robust.

We perform a second experiment to evaluate the capacity of our algorithm to find high-reducibility decompositions. With that aim, we compare our protocol with an alternative decomposition algorithm that we call random algorithm (RA). In RA interactions are randomly selected from the interaction diagram. The experiment, Table II, shows that our algorithm consistently outperforms the random algorithm RA.

(o, N)	(2, 2)	(2, 3)	(2, 4)	(2, 5)	(3, 2)	(3, 3)	(3, 4)
r_{RA}	0.33	0.38	0.42	0.47	0.30	0.33	0.39
r	0.41	0.52	0.57	0.62	0.40	0.46	0.52

TABLE II: Average values of reducibilities r_{RA} computed with a random algorithm and r computed with our method, over 1000 realizations. We decomposed the transition matrices of systems with parameters o, N and $|X_n| = 2$.

We have developed a framework for studying complex systems whose dynamics is ruled by time-ordered and multibody dependencies. The framework is based on interactions, which emerge from the expansion of time-evolution operators for multivariate higher-order Markov chains. We have proposed a measure for the complexity of interaction ensembles and an algorithm to extract them from time series data. We believe these contributions to be a relevant asset for the field of complex systems as they address a currently latent problem by conciliating a data-oriented perspective with a system-dynamics approach.

Authors acknowledge support from the Swiss National Science Foundation via grant SNSF-176938. We also thank Vincenzo Perri for useful comments.

-
- [1] C. W. J. Granger, *Econometrica* **37**, 424 (1969).
- [2] J. Pearl, *Causality: Models, Reasoning, and Inference* (Cambridge University Press, 2000).
- [3] J. Runge, *Chaos* **28**, 075310 (2018).
- [4] R. Albert and A.-L. Barabási, *Rev. Mod. Phys.* **74**, 47 (2002).
- [5] V. Latora, V. Nicosia, and G. Russo, *Complex networks: Principles, methods and applications* (Cambridge University Press, 2017).
- [6] M. Newman, *Networks: An Introduction* (Oxford University Press, 2018).
- [7] M. Kivelä, A. Arenas, M. Barthelemy, J. P. Gleeson, Y. Moreno, and M. A. Porter, *J. Complex Netw.* **2**, 203 (2014).
- [8] S. Boccaletti, G. Bianconi, R. Criado, C. I. del Genio, J. Gómez-Gardeñes, M. Romance, I. Sendiña-Nadal, Z. Wang, and M. Zanin, *Phys. Rep.* **544**, 1 (2014).
- [9] C. Berge, *Hypergraphs: combinatorics of finite sets* (Elsevier, 1984).
- [10] A. Hatcher, *Algebraic Topology* (Cambridge University Press, 2002).
- [11] P. Holme, *Eur. Phys. J. B* **88**, 1 (2015).
- [12] A. R. Benson, D. F. Gleich, and J. Leskovec, *Science* **353**, 163 (2016).
- [13] R. Lambiotte, M. Rosvall, and I. Scholtes, *Nat. Phys.* **15**, 313 (2019).
- [14] F. Battiston, G. Cencetti, I. Iacopini, V. Latora, M. Lucas, A. Patania, J.-G. Young, and G. Petri, *Phys. Rep.* **874**, 1 (2020).
- [15] L. Torres, A. S. Blevins, D. S. Bassett, and T. Eliassirad, *SIAM Rev.* **63** (2021).
- [16] C. Bick, E. Gross, H. A. Harrington, and M. T. Schaub, Preprint (2021).
- [17] F. B. et al, *Nat. Phys.* **17**, 1093 (2021).
- [18] A. A. Markov, *Science in Context* **19**, 591 (2006).
- [19] T. M. Cover and J. A. Thomas, *Elements of Information Theory* (Wiley, 2006).
- [20] Y. Zhang, V. Latora, and A. E. Motter, *Commun. Phys.* **4** (2021).
- [21] S. Chowdary, A. Kumar, G. Cencetti, I. Iacopini, and F. Battiston, *J. Phys. Complex.* **2**, 035019 (2021).
- [22] L. Neuhäuser, R. Lambiotte, and M. T. Schaub, Preprint (2021).
- [23] H. Akaike, *IEEE Trans. Autom. Control* **19**, 716 (1974).
- [24] G. Schwarz, *Ann. Statist.* **6**, 461 (1978).
- [25] I. Scholtes, in *Proceedings of the 23rd ACM SIGKDD international conference on knowledge discovery and data mining* (2017) p. 1037.

SUPPLEMENTAL MATERIAL

a.- Higher-order Markov chains will be able to describe the dynamics of S as long as the following assumptions hold: (1) The same statistical behaviour is expected at all points in time (causal stationarity). (2) No external variables can influence the dynamics of S (causal sufficiency) [3].

b.- An interaction \mathcal{A} of type \mathbf{q} is nested in an interaction \mathcal{A}' of type \mathbf{q}' by fixing the transition probabilities of \mathcal{A}' to those of \mathcal{A} :

$$\pi(\mathbf{G}^{\mathbf{v}'}(t)|G^{\mathbf{h}'}(t-1)) = \frac{\pi(\mathbf{G}^{\mathbf{v}}(t)|\mathbf{G}^{\mathbf{h}}(t-1))}{\prod_{\substack{q'_n \neq 0 \\ q_n = 0}} |X_i|}. \quad (4)$$

c.- We now explain the procedure to extract an interaction at interaction order ω . This procedure has been designed for nodes with all equal alphabets $X_n = X_{n'} \forall n, n' \in \mathcal{N}$. If nodes were different our algorithm would also yield a valid decomposition, but it should be modified for improved results.

First, we randomly select an interaction \mathcal{A} at interaction order ω to obtain its interaction matrix \mathbf{A} . This, models transitions from histories $\bar{y} \in X^{\mathbf{h}}$ to states $y \in X^{\mathbf{v}}$. For every $y \in X^{\mathbf{v}}$ and $\bar{y} \in X^{\mathbf{h}}$, we create a set of matrix elements $\tilde{T}_{x\bar{x}}$ such that states $x \in X$ and $\bar{x} \in X^{\mathbf{m}}$ correspond to the same y and \bar{y} , respectively. The minimum of each such set is the element $R_{y\bar{y}}$ of the auxiliary matrix \mathbf{R} :

$$R_{y\bar{y}} = \min\{\tilde{T}_{x\bar{x}} | \forall y_j, \bar{y}_j \neq \emptyset : y_{jk} = x_{jk}, \bar{y}_{jk} = \bar{x}_{jk}\} \quad (5)$$

where y_{jk} and \bar{y}_{jk} are assumed to go over all k where y_j and \bar{y}_j are not empty, respectively. When all \bar{y}_j are empty, $q_n \leq 1 \forall n$, \mathbf{R} is a $1 \times |X^{\mathbf{v}}|$ matrix, whose values are computed with all columns at \mathbf{T} . If additionally all y_j are also empty, $\mathbf{q} = \mathbf{0}$, \mathbf{R} is a 1×1 matrix corresponding to the smallest matrix element of \mathbf{T} . We then obtain \mathbf{A} by normalizing \mathbf{R} .

In the second step, the interaction \mathcal{A} is represented as an interaction of type \mathbf{o} , and the transition matrix $\hat{\mathbf{A}}$ has the same dimensions as $\tilde{\mathbf{T}}$. We find the maximal value of a such that all elements of $\tilde{\mathbf{T}} - a\hat{\mathbf{A}}$ are non-negative: we compute minimal column sum of \mathbf{R} , and include the uniform distribution for the states of nodes n for which $q_n = 0$.

$$a_i = \left(\min_{\bar{y}} \sum_y R_{y\bar{y}} \right) \prod_{q_j=0} |X_j| \quad (6)$$

If $a = 0$, we start a new iteration with a different interaction. When all interactions at interaction order ω yield $a = 0$ we explore the next interaction order $\omega + 1$.

In the third step we extract the contribution of \mathcal{A} from $\tilde{\mathbf{T}}$: the new value, $\tilde{\mathbf{T}}'$, is given by $\tilde{\mathbf{T}}' = \tilde{\mathbf{T}} - a\hat{\mathbf{A}}$. This sequence of steps is repeated until $\tilde{\mathbf{T}}'$ is a matrix of zeros, or equivalently until $\sum_i a_i = 1$. See the next paragraph for an example.

We have tested a different version of the algorithm where we carry out a more exhaustive search: at each iteration we compute a_i for all available interactions at interaction order ω and then select the interaction with the highest value of a_i . However, such procedure is not able to outperform the main decomposition algorithm despite its computational cost.

d.- Consider the following example of $\tilde{\mathbf{T}}$ in a system with $N = 2$, $o = 2$ and $|X_n| = 2$. We here show an iteration of the decomposition algorithm step by step. The interaction to be extracted will be interaction \mathcal{A} with type $\mathbf{q} = (0, 2)$. Therefore we have $\mathbf{G}^{(2,2)}(t)$ and $\mathbf{G}^{(0,2)}(t)$ to characterize the complete system variables and the interaction variables respectively. The auxiliary matrix \mathbf{R} is obtained from $\tilde{\mathbf{T}}$ as

$$\tilde{T} = \frac{1}{100} \begin{pmatrix} 33 & 22 & 13 & 64 \\ 3 & 34 & 4 & 14 \\ 47 & 2 & 23 & 17 \\ 17 & 42 & 60 & 5 \end{pmatrix} \longrightarrow R = \frac{1}{100} \begin{pmatrix} 13 & 2 \\ 3 & 5 \end{pmatrix} \quad (7)$$

Let us visualize how R_{00} has been computed. R_{00} accounts for $\pi(\mathbf{G}^{(0,1)}(t) = 0 | \mathbf{G}^{(0,1)}(t-1) = 0)$, and is thus associated with the elements of $\tilde{\mathbf{T}}$ that encode the same transition probability complemented with all the possible

values for $\mathbf{G}^{(1,0)}(t)$ and $\mathbf{G}^{(1,0)}(t-1)$:

$$\begin{aligned}\pi(\mathbf{G}_0^1(t) = 0, \mathbf{G}_1^1(t) = 0 | \mathbf{G}_0^1(t-1) = 0, \mathbf{G}_1^1(t-1) = 0) &= 33/100 \\ \pi(\mathbf{G}_0^1(t) = 0, \mathbf{G}_1^1(t) = 0 | \mathbf{G}_0^1(t-1) = 1, \mathbf{G}_1^1(t-1) = 0) &= 13/100 \\ \pi(\mathbf{G}_0^1(t) = 1, \mathbf{G}_1^1(t) = 0 | \mathbf{G}_0^1(t-1) = 0, \mathbf{G}_1^1(t-1) = 0) &= 47/100 \\ \pi(\mathbf{G}_0^1(t) = 1, \mathbf{G}_1^1(t) = 0 | \mathbf{G}_0^1(t-1) = 1, \mathbf{G}_1^1(t-1) = 0) &= 23/100\end{aligned}$$

or in a more compact form

$$\begin{aligned}\pi(\mathbf{G}^{(1,1)}(t) = (0, 0) | \mathbf{G}^{(1,1)}(t-1) = (0, 0)) &= 33/100 \\ \pi(\mathbf{G}^{(1,1)}(t) = (0, 0) | \mathbf{G}^{(1,1)}(t-1) = (1, 0)) &= 13/100 \\ \pi(\mathbf{G}^{(1,1)}(t) = (1, 0) | \mathbf{G}^{(1,1)}(t-1) = (0, 0)) &= 47/100 \\ \pi(\mathbf{G}^{(1,1)}(t) = (1, 0) | \mathbf{G}^{(1,1)}(t-1) = (1, 0)) &= 23/100\end{aligned}$$

The auxiliary matrix is constructed with the minimal of those elements such that when \mathbf{A} is removed from $\tilde{\mathbf{T}}$ no negative elements are created in the next iteration.

The second step yields $a = (2/100 + 5/100) \times 2$, where the first part comes from $R_{01} + R_{11}$, and the second part comes from the dimensions of $|X_0| = 2$.

$$\mathbf{R} = \frac{1}{100} \begin{pmatrix} 13 & 2 \\ 3 & 5 \end{pmatrix} \longrightarrow \mathbf{A} = \begin{pmatrix} \frac{13}{16} & \frac{2}{7} \\ \frac{3}{16} & \frac{5}{7} \end{pmatrix} \quad (8)$$

In the third step we move from a $\mathbf{q} = (0, 2)$ representation of \mathbf{A} to a $\mathbf{q} = (2, 2)$ representation.

$$\begin{pmatrix} \frac{13}{16} & \frac{2}{7} \\ \frac{3}{16} & \frac{5}{7} \end{pmatrix} \longrightarrow \begin{pmatrix} \frac{\frac{13}{2 \times 16}}{\frac{3}{2 \times 16}} & \frac{\frac{2}{2 \times 7}}{\frac{5}{2 \times 7}} & \frac{\frac{13}{2 \times 16}}{\frac{3}{2 \times 16}} & \frac{\frac{2}{2 \times 7}}{\frac{5}{2 \times 7}} \\ \frac{\frac{13}{2 \times 16}}{\frac{3}{2 \times 16}} & \frac{\frac{2}{2 \times 7}}{\frac{5}{2 \times 7}} & \frac{\frac{13}{2 \times 16}}{\frac{3}{2 \times 16}} & \frac{\frac{2}{2 \times 7}}{\frac{5}{2 \times 7}} \\ \frac{\frac{13}{2 \times 16}}{\frac{3}{2 \times 16}} & \frac{\frac{2}{2 \times 7}}{\frac{5}{2 \times 7}} & \frac{\frac{13}{2 \times 16}}{\frac{3}{2 \times 16}} & \frac{\frac{2}{2 \times 7}}{\frac{5}{2 \times 7}} \\ \frac{\frac{13}{2 \times 16}}{\frac{3}{2 \times 16}} & \frac{\frac{2}{2 \times 7}}{\frac{5}{2 \times 7}} & \frac{\frac{13}{2 \times 16}}{\frac{3}{2 \times 16}} & \frac{\frac{2}{2 \times 7}}{\frac{5}{2 \times 7}} \end{pmatrix} \quad (9)$$

At this point it becomes clear that the correction in the dimension at SM Eq. (6) is necessary to normalize the $q_n = o$ form of \mathbf{A} to model nodes with $q_n = 0$.

e.- We organize the transition probabilities of the model in a transition matrix \mathbf{W} ordered according to \mathcal{B} . The output matrices \mathbf{U} and \mathbf{V} , with dimensions $u_r \times u_c$ and $v_r \times v_c$ read

$$U_{nm} = \sum_{i=0}^{v_c-1} W_{nv_r+i, mv_c} \quad V_{nm} = \sum_{i=0}^{u_c-1} W_{iv_r+n, m} \quad (10)$$

If $\mathbf{W} = \mathbf{U} \otimes \mathbf{V}$ holds \mathbf{U} and \mathbf{V} are valid subsystem interaction matrices. In that case, the procedure should be applied again on \mathbf{U} and \mathbf{V} until no more subsystems can be isolated. For an interaction \mathcal{A} of type \mathbf{q} subsystem interactions at nodes \mathcal{B} have $\prod_{n \in \mathcal{B}} |X_n|^{q_n}$ parameters, and the decomposed interaction has only $\sum_{\mathcal{B}} \prod_{n \in \mathcal{B}} |X_n|^{q_n}$ degrees of freedom.

Let \mathbf{A} be the transition matrix of an interaction with $N = 2$, $|X_0| = 3$ and $|X_1| = 2$. Our goal here is to decompose \mathbf{A} as $\mathbf{A} = \mathbf{U} \otimes \mathbf{V}$ with $\mathbf{U} \in \mathbb{R}^{3 \times 3}$ and $\mathbf{V} \in \mathbb{R}^{2 \times 2}$. If we assumed $\mathbf{U} \otimes \mathbf{V}$ the following would hold:

$$\begin{pmatrix} u_{00} & u_{01} & u_{02} \\ u_{10} & u_{11} & u_{12} \\ u_{20} & u_{21} & u_{22} \end{pmatrix} \otimes \begin{pmatrix} v_{00} & v_{01} \\ v_{10} & v_{11} \end{pmatrix} = \begin{pmatrix} u_{00}v_{00} & u_{00}v_{01} & u_{01}v_{00} & u_{01}v_{01} & u_{02}v_{00} & u_{02}v_{01} \\ u_{00}v_{10} & u_{00}v_{11} & u_{01}v_{10} & u_{01}v_{11} & u_{02}v_{10} & u_{02}v_{11} \\ u_{10}v_{00} & u_{10}v_{01} & u_{11}v_{00} & u_{11}v_{01} & u_{12}v_{00} & u_{12}v_{01} \\ u_{10}v_{10} & u_{10}v_{11} & u_{11}v_{10} & u_{11}v_{11} & u_{12}v_{10} & u_{12}v_{11} \\ u_{20}v_{00} & u_{20}v_{01} & u_{21}v_{00} & u_{21}v_{01} & u_{22}v_{00} & u_{22}v_{01} \\ u_{20}v_{10} & u_{20}v_{11} & u_{21}v_{10} & u_{21}v_{11} & u_{22}v_{10} & u_{22}v_{11} \end{pmatrix} \quad (11)$$

It is possible to invert the tensor operation by using the property that both \mathbf{U} and \mathbf{V} are stochastic, and therefore sums over columns of \mathbf{V} or \mathbf{U} contained in \mathbf{A} are cancelled out and can be used to isolate the remaining variable.

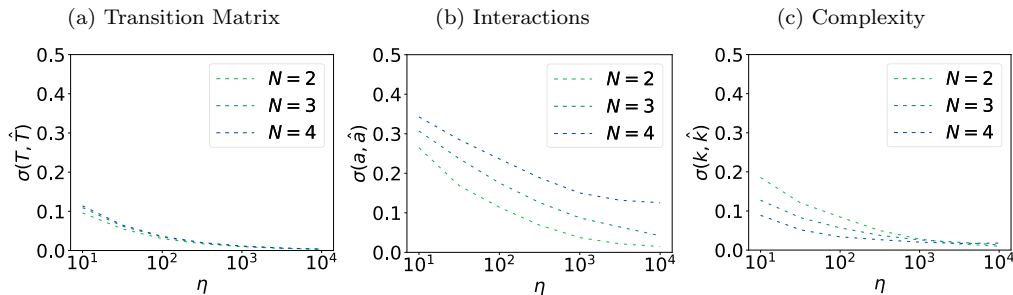


FIG. 5: We produce synthetic sequences with length $L = \eta \prod_{n \in \mathcal{N}} |X_n|^o$ and compute the total variation distance σ as a function of η between the original (a) transition matrices (b) interactions (c) weights, and the ones inferred from the data for a fixed alphabet $|X_n| = 2$ and order $o = 3$. Results reported here correspond to averages over 100 realizations for each (η, N) tuple.

As an example one may obtain $U_{00} = A_{00} + A_{10}$ and also as $U_{00} = A_{10} + A_{11}$. The same is true for \mathbf{V} as $V_{00} = A_{00} + A_{20} + A_{40}$, $V_{00} = A_{02} + A_{22} + A_{42}$ and $V_{00} = A_{04} + A_{24} + A_{44}$. Since these equations are redundant, one may pick one at random and discard the rest. The expression at SM Eq. (10) selects always the first one. This technique will always output a \mathbf{U}, \mathbf{V} pair even if the tensor factorization does not exist. Therefore one should always check whether $\mathbf{A} = \mathbf{U} \otimes \mathbf{V}$ holds. For the purpose of finding subsystem interactions, we recursively apply this procedure on different combinations of interaction partitions until no more subsystem interactions can be found.

f.- In this paragraph we prove that r is the fraction of the area behind $k^c(l)$. From the definition of $k(l) = \sum_{\lambda(\mathcal{A}^i)=l} a_i$ we could obtain the cumulative as $k^c(l) = \sum_{\lambda(\mathcal{A}^i) \leq l} a_i$. Instead, we are going to express the k as a function of a continuous variable $\phi \in [0, \lambda_{\text{MC}}]$ as $k = \sum a_i \delta(\phi - \lambda(\mathcal{A}^i))$. Then the cumulative $k^c(\phi)$ is

$$k^c(\phi) = \int_0^\phi k(\phi') d\phi' = \int_0^\phi \sum a_i \delta(\phi' - \lambda(\mathcal{A}^i)) d\phi' = \sum a_i \int_0^\phi \delta(\phi' - \lambda(\mathcal{A}^i)) d\phi' = \sum a_i \theta(\phi - \lambda(\mathcal{A}^i)) \quad (12)$$

Now the area behind $k^c(\phi)$ is

$$\int_0^{\lambda_{\text{MC}}} k^c(\phi) d\phi = \int_0^{\lambda_{\text{MC}}} \sum a_i \theta(\phi - \lambda(\mathcal{A}^i)) d\phi = \sum a_i \int_0^{\lambda_{\text{MC}}} \theta(\phi - \lambda(\mathcal{A}^i)) d\phi = \sum a_i \int_{-\lambda(\mathcal{A}^i)}^{\lambda_{\text{MC}} - \lambda(\mathcal{A}^i)} \theta(\phi') d\phi' \quad (13)$$

$$= \sum a_i (\lambda_{\text{MC}} - \lambda(\mathcal{A}^i)) = \lambda_{\text{MC}} - \sum a_i \lambda(\mathcal{A}^i) \quad (14)$$

The total area is simply λ_{MC} , therefore the share is obtained by dividing the expression above with λ_{MC} , which yields exactly r .

g.- We show two additional experiments to validate the robustness of our algorithm to extract interactions from data. First we replicate the experiment in the main text with a different order of $o = 3$, see SM Fig. 5. The results are aligned with those in the main text, and show that one can obtain a reducible ensemble of interactions with a good predicting capacity even when there is not enough data to accurately infer the ground truth interactions.

We have carried out a second experiment to explore alphabets with $|X_n| \neq 2$. The procedure is the same as the one explained in the main text: we first randomly generate a transition matrix \mathbf{T} and extract the ground truth values for interaction coefficients a and weights k . We then create sequences of length $L = \eta \prod_{n \in \mathcal{N}} |X_n|^o$ from \mathbf{T} , and use them to infer $\hat{\mathbf{T}}$. We apply our algorithm to $\hat{\mathbf{T}}$ and obtain \hat{a} and \hat{k} . We run 100 simulations for each different (X, N, o) tuple. See the results in SM Fig. 6.

We observe again the trend explained in the main text: despite interactions being very susceptible to statistical errors, the weights are not. This implies that when studying the dynamics of a time-ordered and many-body system, the reducibility of inferred interaction decomposition will be close to the correct value even if interaction themselves are different.

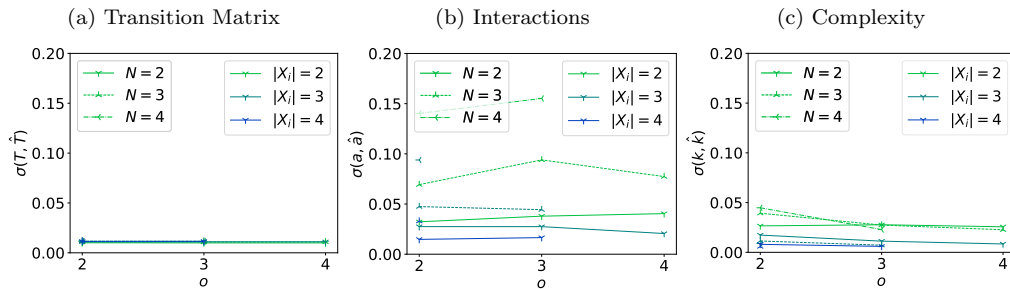


FIG. 6: We produce synthetic sequences with length $L = \eta \prod_{n \in \mathcal{N}} |X_n|^o$ and compute the total variation distance σ between the original (a) transition matrices (b) interactions (c) weights, and the ones inferred from the data for a fixed $\eta = 1000$. Results reported here correspond to averages over 100 realizations for each (X, N, o) tuple.

h.- We use our formalism to study transportation bottlenecks in the city of Sao Paulo between January 2010 and September 2018. The system is encoded in $N = 5$ nodes with $|X_n| = 2$ representing to the presence or absence of a traffic jam in the corresponding region of the city: $\{west, south, east, centre, north\}$. The dataset provides a record of traffic congestion events with a resolution of 30 minutes, that we have transformed into a timeline of $L = 153268$ states by using the alphabet $\{\text{no jam} \rightarrow 0, \text{jam} \rightarrow 1\}$ for each node. We then create the joint state and apply our machinery to decompose the transition matrix in interactions. Based on $L = \eta \prod_{i \in \mathcal{N}} |X_i|^o$, we set $o^+ = 5$ and $\eta \sim 150$ as the maximum value of o and associated scale factor, which should yield values of σ in the order of 0.3 and 0.1 for the interactions and for the ensemble weights respectively. The AIC estimation yields a value of $o = 2$, for the multibody Markov chain.

Results in SM Fig. 7 show how the system is mainly dominated by \mathcal{A} with type $q_n = 2$. A closer look at the interaction's transition matrix reveals the most important trajectories at the phase space: We have $\mathbf{s}(t-1) = (0, 0, 0, 0, 0) \rightarrow \mathbf{s}(t) = (0, 0, 0, 0, 0)$, $\mathbf{s}(t-1) = (1, 1, 1, 1, 0) \rightarrow \mathbf{s}(t) = (1, 1, 1, 1, 0)$ and $\mathbf{s}(t-1) = (1, 1, 1, 1, 1) \rightarrow \mathbf{s}(t) = (1, 1, 1, 1, 1)$ amongst the processes with a higher probability to occur, where the three of them express a situation in which the system remains in the same state. Next on the list we have $\mathbf{s}(t-1) = (1, 1, 1, 1, 0) \rightarrow \mathbf{s}(t) = (1, 1, 1, 1, 1)$, $\mathbf{s}(t-1) = (1, 1, 1, 1, 1) \rightarrow \mathbf{s}(t) = (1, 1, 1, 1, 0)$ and $\mathbf{s}(t-1) = (1, 1, 1, 1, 0) \rightarrow \mathbf{s}(t) = (1, 1, 0, 1, 0)$. The first two account respectively for the propagation of a traffic jam to the north of the city when the rest of locations are also collapsed and the opposite process. The latter expresses a traffic dispersion in the east when all but the north are collapsed. Finally, despite a of $q_n = 2$ being the largest coefficient by far, the rest are not negligible which yields a reducibility of $r = 0.26$.

i.- We have analysed a compilation of the 18 major pieces of the Well-Tempered Clavier by J.S. Bach. The possible node states are the sound or silence, $|X_n| = 2$, of the tonic, third and fifth notes of the scale, $N = 3$. For a maximum value of o given by $o^+ = 5$ the AIC establishes a value of $o = 4$ for this dataset composed by $L = 3541898$ events, which yields $\eta = 864.721$ and an associated $\sigma < 0.1$ if we extrapolate the numerical results from the experiment in the main text. See the outcome of the study at SM Fig. 7.

Interaction coefficients at SM Fig. 7 shed light on a bicephalous character of the system with $\mathbf{q} = (2, 2, 2)$ and $\mathbf{q} = (4, 4, 4)$ as leading interaction types. Let us focus on $\mathbf{q} = (2, 2, 2)$ which is slightly more influential: The interaction's transition matrix is exactly the identity matrix of dimension $|X|$, which represents a simple static process. This identity matrix can be written as a tensor product of three identity matrices of dimension $|X_n| = 2$. Therefore, we have an interaction whose coefficient is high, and whose number of parameters $\lambda(\mathcal{A})$ is small, which results in a large reducibility of $r = 0.64$ for the whole system. We argue that the prevalence of the interaction type with $\mathbf{q} = (2, 2, 2)$ and the overall reducible character of the system are a direct consequence of the time resolution of the dataset \mathbf{D} . We have obtained \mathbf{D} by translating midi files, for which two consecutive time steps are separated only a tiny fraction of the duration of average notes. Thus, repetition is the standard behaviour expected in the system.

j.- We have realized a last proof of principle experiment to support the need of our formalism over current methods for describing time-ordered interactions (single variable higher-order Markov chains) and multibody interactions (hypergraphs). We train the three models with musical data from the Well-Tempered Clavier introduced in the previous paragraph. Let us explain in more detail the experimental setup and the results for each model:

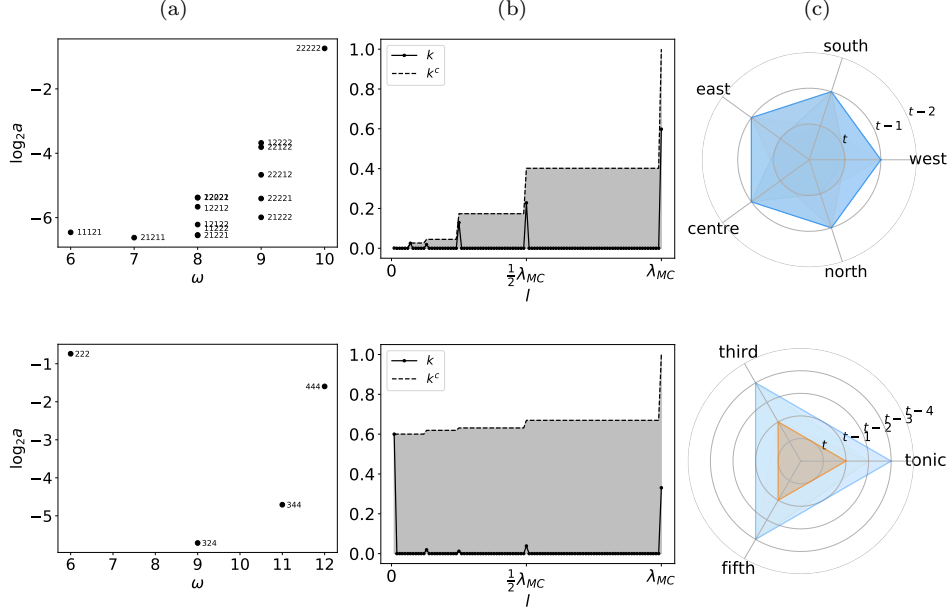


FIG. 7: We report the results of our analysis of Traffic jams and Musical compositions in the first and second rows. (a) Selection of dominant interactions with $a > 0.01$ whose coefficients are plotted on a logarithmic scale and are labelled with the corresponding interaction type \mathbf{q} . (b) Weights and reducibility. (c) We represent most relevant interactions with their \mathbf{q} in a polar plot where the radial and angular coordinates account for q_n and n respectively. The opacity of each interaction corresponds to its interaction coefficient.

- Multi-time and not multi-body: We train a standard higher-order Markov chain with memory $m = 3$ in each of the $N = 3$ nodes and compute the log-likelihood function. We then add the values obtained for each node under the assumption that the joint dynamics doesn't have multibody contributions.

- Multi-body and not multi-time: Ideally we should find the hypergraph model that best describes the time-aggregated dynamics of the system. In other words, we compute $\pi(\mathbf{s}(t)|\mathbf{s}(t-1))$ with the $\mathbf{s}(\tau-1) \rightarrow \mathbf{s}(\tau)$ statistics $\forall \tau$. Notice that this corresponds to interaction type $\mathbf{q} = (1, 1, 1)$ in our formalism, or equivalently to a standard Markov chain with $m = 1$ on the joint node state $\mathbf{s}(t)$. Therefore, the performance of any hypergraph model we can think of will be upper bounded by the performance of $\mathbf{q} = (1, 1, 1)$. We thus compute the log-likelihood for the Markov chain and use that to characterize the best possible representative of multi-body and not multi-time models.

- Multi-body and multi-time: We compute the same multivariate higher-order markov chain for the joint node state $\mathbf{s}(t)$ with $m = 3$ presented in the previous example.

The log-likelihoods of each model yield $(-798119, -149767, -144254)$. The better value for the third case was expected from the number of parameters each model has available. However, let us note that time-ordered multibody interactions are precisely introduced to optimize the number of parameters. In this case the formalism identifies that an important contribution comes from the interaction type $\mathbf{q} = (1, 1, 1)$ allowing a more parsimonious understanding while preserving a better prediction capacity.